IAI Journals.ASM.org

# Free Lipid A Isolated from *Porphyromonas gingivalis* Lipopolysaccharide Is Contaminated with Phosphorylated Dihydroceramide Lipids: Recovery in Diseased Dental Samples

**Frank C. Nichols,[a] Bekim Bajrami,[b] Robert B. Clark,[c] William Housley,[c] and Xudong Yao[b]**

Department of Oral Health and Diagnostic Sciences, University of Connecticut School of Dental Medicine, Farmington, Connecticut, USA[a]; Department of Chemistry, University of Connecticut, Storrs, Connecticut, USA[b]; and Department of Immunology, University of Connecticut School of Medicine, Farmington, Connecticut, USA[c]

**Recent reports indicate that *Porphyromonas gingivalis* mediates alveolar bone loss or osteoclast modulation through engagement of Toll-like receptor 2 (TLR2), though the factors responsible for TLR2 engagement have yet to be determined. Lipopolysaccharide (LPS) and lipid A, lipoprotein, fimbriae, and phosphorylated dihydroceramides of *P. gingivalis* have been reported to activate host cell responses through engagement of TLR2. LPS and lipid A are the most controversial in this regard because conflicting evidence has been reported concerning the capacity of *P. gingivalis* LPS or lipid A to engage TLR2 versus TLR4. In the present study, we first prepared *P. gingivalis* LPS by the Tri-Reagent method and evaluated this isolate for contamination with phosphorylated dihydroceramide lipids. Next, the lipid A prepared from this LPS was evaluated for the presence of phosphorylated dihydroceramide lipids. Finally, we characterized the lipid A by the matrix-assisted laser desorption ionization mass spectrometry (MALDI-MS) and electrospray-MS methods in order to quantify recovery of lipid A in lipid extracts from diseased teeth or subgingival plaque samples. Our results demonstrate that both the LPS and lipid A derived from *P. gingivalis* are contaminated with phosphorylated dihydroceramide lipids. Furthermore, the lipid extracts derived from diseased teeth or subgingival plaque do not contain free lipid A constituents of *P. gingivalis* but contain substantial amounts of phosphorylated dihydroceramide lipids. Therefore, the free lipid A of *P. gingivalis* is not present in measurable levels at periodontal disease sites. Our results also suggest that the TLR2 activation of host tissues attributed to LPS and lipid A of *P. gingivalis* could actually be mediated by phosphorylated dihydroceramides.**

*Porphyromonas gingivalis*, along with many other potential periodontal pathogens, produce virulence factors capable of promoting tissue inflammation, loss of connective tissue attachment, and bone loss. Lipopolysaccharide (LPS) and lipid A are extensively studied microbial virulence factors from the standpoint of periodontal disease pathogenesis (1, 4, 9, 10, 20, 23, 24, 34–36, 38, 40), and both can promote inflammatory reactions and bone loss characteristic of tissue changes observed in chronic periodontitis. However, LPS or lipid A of *P. gingivalis* has not been demonstrated in diseased periodontal tissues. Instead, we reported that a unique fatty acid constituent of both lipid A and LPS of *P. gingivalis*, called 3-hydroxy isobranched $C_{17:0}$ (3-OH iso $C_{17:0}$), exists in lipid products recovered predominantly from organic solvent extracts of subgingival plaque, periodontally diseased tissues, and diseased teeth, with little recovered in aqueous extracts of these samples (26, 29). Since LPS partitions essentially only into the aqueous phase with this extraction technique (39), we concluded that LPS of *P. gingivalis* and other related *Bacteroidetes* bacteria (33), including *Prevotella intermedia* and *Tannerella forsythia*, is not present to a significant extent in diseased periodontal tissues. By analogy, it is presumed that LPS from non-*Bacteroidetes* subgingival organisms also does not contaminate diseased periodontal tissues. We have since shown that organic solvent extracts of diseased periodontal tissues contain phosphorylated dihydroceramide (PDHC) lipids of *P. gingivalis* (32, 33). These phosphorylated dihydroceramide lipids contain 3-OH iso $C_{17:0}$. In contrast, the free lipid A of *P. gingivalis*, which is soluble in organic solvent, also contains 3-OH iso $C_{17:0}$ as a fatty acid constituent. The possibility exists that the 3-OH iso $C_{17:0}$ recovered from organic extracts of subgingival plaque samples and periodontally diseased tissues could include free lipid A species devoid of the O-polysaccharide component of LPS. The first aim of this investigation was to isolate lipid A from *P. gingivalis*, and after characterization of the molecular structures using matrix-assisted laser desorption ionization tandem mass spectrometry (MALDI-MS/MS) and electrospray-MS/MS, we determined whether the dominant phosphorylated lipid A species are present in lipid extracts of periodontally diseased teeth and subgingival plaque samples.

The phosphorylated dihydroceramide lipid classes of *P. gingivalis* that promote proinflammatory reactions and morphological changes in fibroblasts (31) are also readily detected on periodontally diseased teeth (32) and are recovered from gingival tissue samples from periodontitis sites (26, 32, 33). This observation is important because the phosphorylated dihydroceramide lipids of *P. gingivalis* are reported to engage Toll-like receptor 2 (TLR2) when promoting dendritic cell secretion of interleukin-6 (IL-6) (29) and inhibiting osteoblast function and mineral deposition *in vivo* and *in vitro* (43). Other reports indicate that *P. gingivalis* mediates bone loss in experimental animals in a TLR2-dependent

**Received** 14 October 2011 **Returned for modification** 31 October 2011
**Accepted** 22 November 2011
**Published ahead of print** 5 December 2011
**Editor:** A. J. Bäumler
Address correspondence to Frank C. Nichols, nichols@nso.uchc.edu.

doi:10.1128/IAI.06180-11

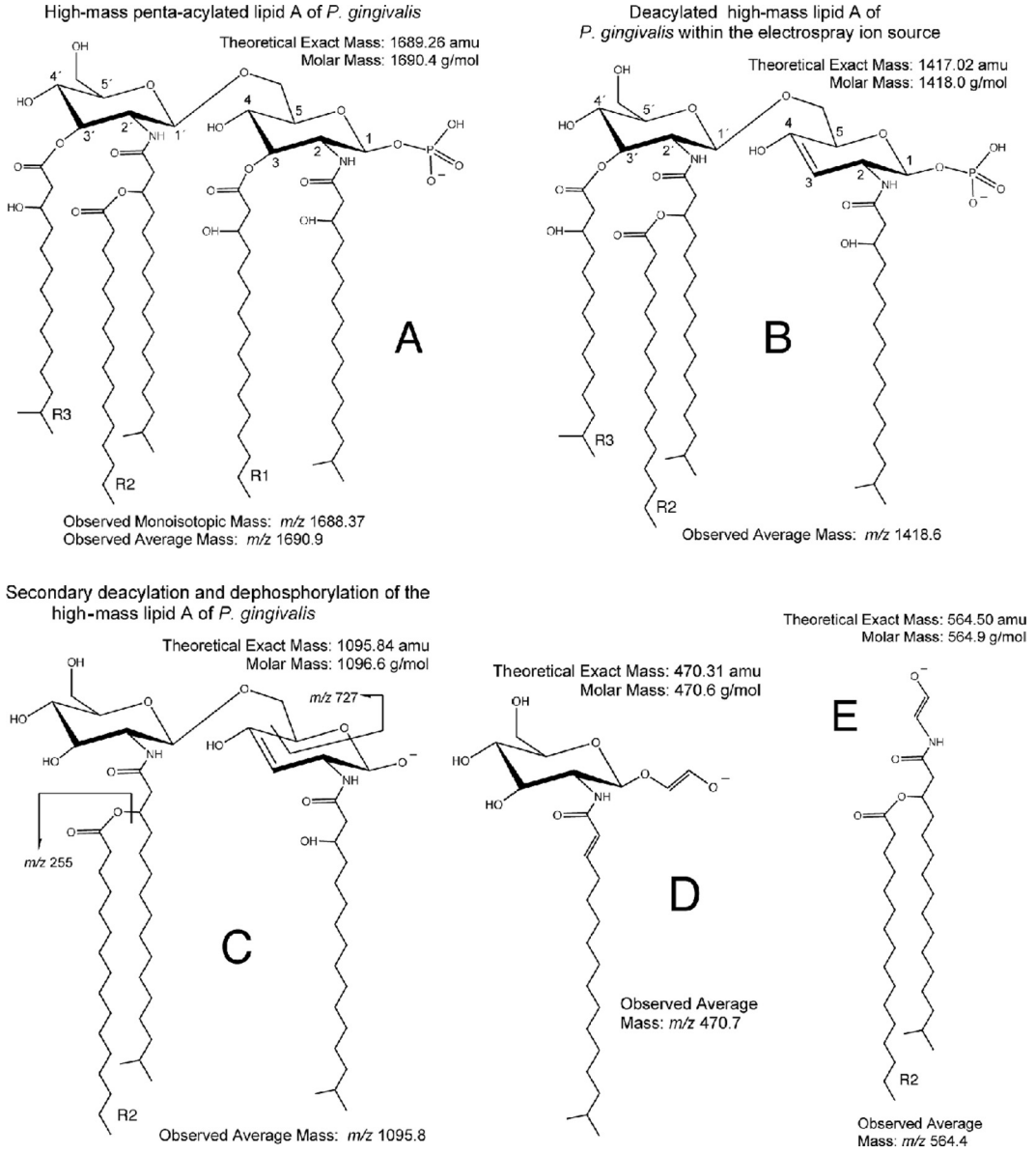


**FIG 1** Structure of the high-mass lipid A of *P. gingivalis* (*m/z* 1,690 negative ion) and its ion fragments. (A) This lipid A negative ion is shown with the phosphate group in the 1 position. Shown is the theoretical exact mass (1,689.26 amu) and theoretical molar mass (1,690.4 g/mol) of this lipid A ion. The observed monoisotopic ion mass was based on the time of flight (TOF)-generated mass spectrum (Fig. 2A), whereas the observed average mass is based on the quadrupole-generated mass spectrum (Fig. 5A). (B) With ESI-MS analysis, the first deacylation/desaturation occurs before entry into the first quadrupole (Q1) and produces a negative ion with an average mass of *m/z* 1,418.6. Additional fatty acids may substitute into lipid A, as shown in Table 2. (C, D, and E) The remaining ion fragments with their respective average ion masses result from collision-induced dissociation. Other fatty acid substitutions for related lipid A ion fragments are listed in Table 3.

manner (14, 15), and a recent report shows that *P. gingivalis* modulates osteoclastogenesis *in vitro* through TLR2 engagement, resulting in differential induction of NFATc1 and NF-κB (47). Though most evidence indicates that bacterial LPS engages only TLR4, the LPS and lipid A of *P. gingivalis* have been reported to act through TLR4 and TLR2 (11, 21, 22) or to interfere with TLR4 responses (42). Therefore, concern exists that TLR2 effects attributed to LPS or lipid A of *P. gingivalis* may actually be accounted for by contaminating TLR2 ligands, such as phosphorylated dihydroceramide lipids. Using the MALDI- and electrospray-MS approaches, the second aim of this study was to determine whether *P. gingivalis* LPS extracted by the Tri-Reagent method or the free lipid A derived from this LPS is contaminated with phosphorylated dihydroceramide lipids.

## MATERIALS AND METHODS

*P. gingivalis* (ATCC 33277) was grown in brain heart infusion broth as previously described (31). LPS was extracted from samples of a lyophilized *P. gingivalis* bacterial pellet using the Tri-Reagent method of Yi and Hackett (46). The crude LPS was subjected to Bligh and Dyer phospholipid extraction (6) prior to precipitation of the LPS with cold magnesium chloride in 95% ethanol (46). After three additional precipitations with 95% ethanol followed by precipitation with 100% ethanol (46), the lyoph-

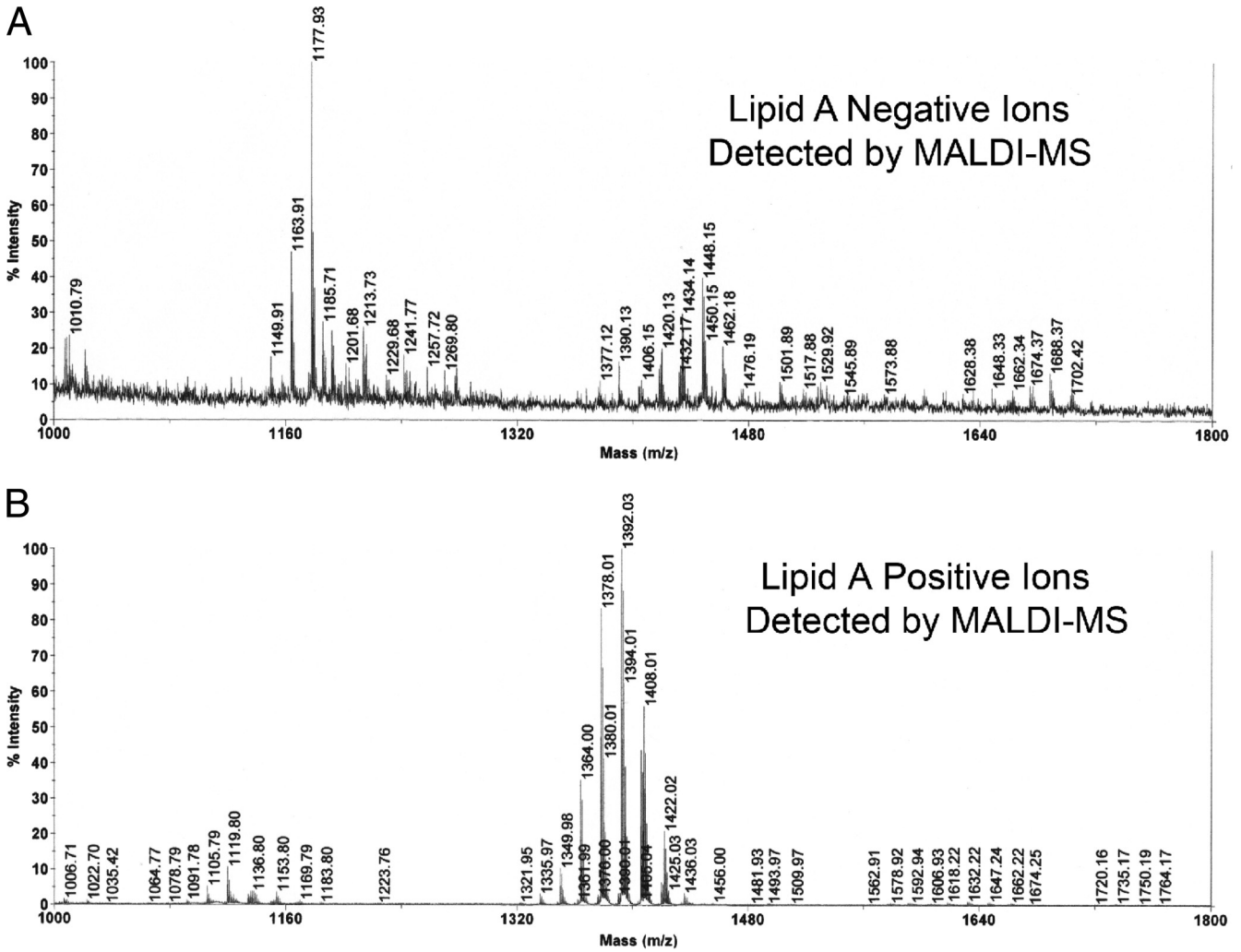


**FIG 2** Negative and positive ions of lipid A produced with MALDI-MS. Lipid A (10 $\mu$g) was combined with CMBT matrix and applied so that approximately 2 $\mu$g was spotted to the steel target plate. Though identical amounts of lipid A were analyzed for each spectrum, negative ions of lipid A, representing phosphorylated lipid A species (A), were recovered in relatively low abundances compared with positive ions of lipid A, representing the nonphosphorylated lipid A species (B).

ilized LPS was subjected to two sequential Bligh and Dyer extractions. Each of the Bligh and Dyer extracts were subjected to electrospray ionization (ESI)-multiple reaction monitoring (MRM) analysis for phosphorylated dihydroceramide lipids as described below. Another sample of the *P. gingivalis* bacterial pellet was extracted using the procedure of Yi and Hackett, including all ethanol precipitation steps (46), the resultant lyophilized LPS was hydrolyzed using the method of Caroff et al. (7), and lipid A was recovered by extraction into hexane-isopropanol-water (6:8:0.75, vol/vol/vol). A sample of lipid A was hydrolyzed to determine ester-linked fatty acids. Lipid A was treated with sodium methoxide (0.5 N $NaOCH_3$ in dry methanol at 0.5 ml for 20 min at 40°C), and the released fatty acid methyl esters were recovered in hexane. Electron impact gas chromatography-MS (GC-MS) combined with selected ion monitoring was used to quantify fatty acid methyl esters. Retention times of synthetic fatty acid methyl esters determined whether ester-linked fatty acids of lipid A were straight or branched chain in configuration. An additional sample of lipid A was hydrolyzed in 4 N KOH (100°C, 3 h), and the recovered total fatty acids were treated to form trimethylsilyl (TMS) ether, pentafluorobenzyl (PFB) ester derivatives (26, 27). In order to account for background free fatty acid present in lipid A, a duplicate lipid A sample was treated directly to form TMS, PFB derivatives. These samples were analyzed by negative-ion GC-MS using previously published methods (26, 27).

For matrix-assisted laser desorption ionization–time of flight mass spectrometry (MALDI-TOF MS) (Applied Biosystems 4700; Keck Biotechnology Resource Laboratory, Yale University School of Medicine, New Haven, CT), lipid A was dissolved in matrix solution (10 $\mu$g lipid A in 20 $\mu$l of 2% 5-chloro-2-mercaptobenzothiazole [CMBT] [5, 8] in hexane-isopropanol-water [6:8:0.75, vol/vol/vol]). For MALDI analysis, the lipids were spotted (approximately 2 $\mu$g/spot) on a steel target plate and dried before analysis. MALDI-MS was used to characterize both positive and negative lipid A ions. MALDI-MS/MS analyses used postsource ion decay for generation of fragment ions. MALDI-MS/MS was performed only for the most abundant positive ions identified in the lipid A isolate. The high-mass negative ions of lipid A identified by MALDI-MS were not evaluated for MS/MS fragmentation due to the low abundances of these ions.

ESI-MS, performed with a QTrap 4000 instrument (AB Sciex), was used to evaluate negative ions of *P. gingivalis* lipid A. Instrument parameters were optimized for the detection of lipid A species for both single-stage MS analysis as well as MS/MS analyses. The ion transitions identified with MS/MS analysis were then used to perform MRM-MS analyses of phosphorylated lipid A species. Instrument parameters for quantifying

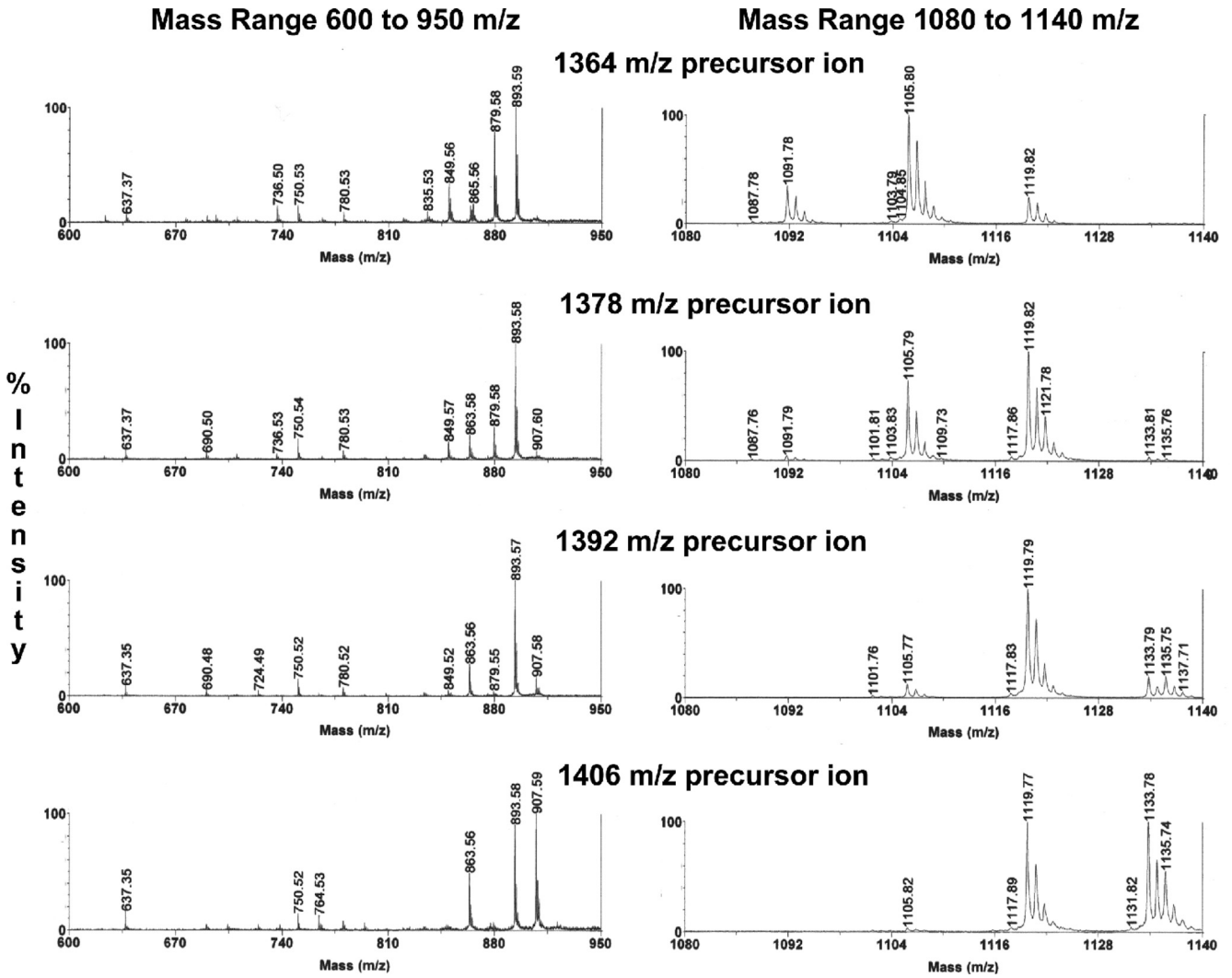


**FIG 3** MALDI-MS/MS of dominant nonphosphorylated lipid A species (positive ions). The dominant nonphosphorylated lipid A species (*m/z* 1,406, 1,392, 1,378, and 1,364) were evaluated by MALDI-MS/MS. The product ions produced from these precursor ions are depicted for the mass range *m/z* 600 to 950 (left) and *m/z* 1,080 to 1,140 (right). Refer to Table 1 for the predicted fatty acid substitutions for these lipid A species as well as other nonphosphorylated lipid A species.

the phosphorylated dihydroceramide lipids were the same as those previously published (33).

Informed consent was obtained from patients in accordance with the Institutional Review Board policy of the University of Connecticut Health Center before donation of teeth or subgingival plaque samples. Teeth and subgingival plaque samples were recovered as previously described (32). Diseased teeth and subgingival plaque samples were taken from sites demonstrating chronic severe periodontitis as described below. Chronic severe periodontitis sites demonstrated greater than 50% alveolar bone loss, periodontal pocket depth of at least 5 mm, bleeding on probing, and substantial mineralized deposits (subgingival calculus) on the tooth roots. Subgingival plaque samples were obtained by placing coarse endodontic paper points into each diseased sulcus and collecting the subgingival plaque contents for approximately 10 seconds. The teeth or subgingival plaque samples were combined from individual donors, and the pooled samples were extracted separately from each donor. Gross adherent soft tissue was removed from calculus-contaminated teeth before lipid extraction, but some adherent soft tissue remained attached to the teeth. Lipids were extracted from dental samples using a modification of the phospholipid extraction procedures of Bligh and Dyer (6) and Garbus et al. (13), and after drying under nitrogen, the lipid extracts were stored frozen until analysis. For MALDI-MS, the lipid extracts of dental samples were dissolved in hexane-isopropanol-water (6:8:0.75, vol/vol/vol) containing the CMBT matrix and spotted as described above. For ESI-MS analyses, the lipid samples were dissolved in hexane-isopropanol-water (6:8:0.75, vol/vol/vol) and were infused directly into the QTrap 4000 instrument at a flow rate of 80 $\mu$l/min (33).

## RESULTS

**Fatty acids recovered from lipid A of *P. gingivalis*.** We first evaluated ester-linked fatty acids in the lipid A of *P. gingivalis* by utilizing the base-catalyzed formation of fatty acid methyl esters. Sodium methoxide treatment followed by GC-MS analysis revealed four saturated fatty acid methyl esters derived from the lipid A preparation of *P. gingivalis*, including isobranched (iso) $C_{17:0}$ (13.5%), $C_{16:0}$ (76.7%), iso $C_{15:0}$ (7.3%), and $C_{14:0}$ (2.6%). Based on previously proposed structures of *P. gingivalis* lipid A (23, 34, 37) and our analysis (see below), these fatty acids will substitute in the R2 position (Fig. 1A). Sodium methoxide treatment of lipid A generated the following hydroxy fatty acid methyl esters: 3-OH iso $C_{17:0}$ (13.0%), 3-OH $C_{16:0}$ (53.6%), 3-OH iso

**TABLE 1** Reconciliation of fatty acid composition of nonphosphorylated lipid A species recovered from *P. gingivalis* LPS[a]

| Precursor ion (recovered as a sodium adduct) | First deacylated ion mass[c] | Resulting from loss of fatty acid (R1) | Loss of *m/z* 227 fragment from 3-OH $C_{17:0}$[d] | Second deacylated ion mass[e] | Resulting from loss of second fatty acid (R2) |
|---|---|---|---|---|---|
| *m/z* 1,364 | *m/z* 1,120 | 3-OH $C_{14:0}$ | *m/z* 894 | *m/z* 637 | $C_{16:0}$ |
| | *m/z* 1,106 | 3-OH iso $C_{15:0}$ | *m/z* 880 | *m/z* 637 | Iso $C_{15:0}$ |
| | *m/z* 1,092 | 3-OH $C_{16:0}$ | *m/z* 866 | *m/z* 637 | $C_{14:0}$ |
| *m/z* 1,378 | *m/z* 1,120 | 3-OH iso $C_{15:0}$ | *m/z* 894 | *m/z* 637 | $C_{16:0}$ |
| | *m/z* 1,106 | 3-OH $C_{16:0}$ | *m/z* 880 | *m/z* 637 | Iso $C_{15:0}$ |
| *m/z* 1,392 | *m/z* 1,134 | 3-OH iso $C_{15:0}$ | *m/z* 908 | *m/z* 637 | Iso $C_{17:0}$ |
| | *m/z* 1,120[b] | 3-OH $C_{16:0}$ | *m/z* 894[b] | *m/z* 637 | $C_{16:0}$ |
| | *m/z* 1,106 | 3-OH iso $C_{17:0}$ | *m/z* 880 | *m/z* 637 | Iso $C_{15:0}$ |
| *m/z* 1,406 | *m/z* 1,134 | 3-OH $C_{16:0}$ | *m/z* 908 | *m/z* 637 | Iso $C_{17:0}$ |
| | *m/z* 1,120 | 3-OH iso $C_{17:0}$ | *m/z* 894 | *m/z* 637 | $C_{16:0}$ |

[a] The lipid A preparation of *P. gingivalis* was subjected to MALDI-MS/MS, and the observed ion fragments shown in Fig. 3 were used to reconcile the loss of fatty acids from these lipid A species. The listed precursor ions represent nonphosphorylated, tetra-acylated lipid A species that deacylate under MALDI-MS/MS in both the R1 and R2 positions with loss of the indicated fatty acids. Note that the second deacylation from the R2 position produces mostly one product ion for all precursor ions listed (*m/z* 637). Additional nonphosphorylated lipid A ions appear as sodium adducts, with masses of *m/z* 1,350, 1,336, and 1,322 (Fig. 2B). However, these lower-mass ions were recovered in low abundance, and MS/MS analysis was not feasible.

[b] Dominant ion transitions noted with MS/MS transitions (see Fig. 4B, C, and D).

[c] See Fig. 4B.

[d] See Fig. 4C.

[e] See Fig. 4D.

$C_{15:0}$ (29.8%), and 3-OH $C_{14:0}$ (3.6%). According to previous reports (23, 34), these fatty acids can exist in the R1 or R3 position of lipid A (Fig. 1A). Analysis of the total hydroxy fatty acids confirmed that 3-OH iso $C_{15:0}$, 3-OH $C_{16:0}$, and 3-OH iso $C_{17:0}$ are the dominant hydroxy fatty acids recovered from *P. gingivalis* lipid A.

**Phosphorylated dihydroceramide lipids recovered from LPS of *P. gingivalis*.** LPS of *P. gingivalis*, extracted by the Tri-Reagent method of Yi and Hackett (46), was subjected to three Bligh and Dyer extraction procedures in order to determine the residual phosphorylated dihydroceramide contamination. The first phospholipid extraction occurred prior to the ethanol washes of the LPS, and two additional phospholipid extractions occurred after the multiple ethanol wash steps of the procedure of Yi and Hackett (46). Phosphorylated dihydroceramides were detected by MRM-MS in all phospholipid extracts (data not shown). Although the third phospholipid extract of LPS contained approximately 25-fold less contaminating dihydroceramide lipids than the first extract of LPS, the levels of contaminating dihydroceramide lipids in the third phospholipid extract were substantial. Given this level of contamination of LPS with phosphorylated dihydroceramide lipids, we next isolated lipid A from *P. gingivalis* LPS, and after characterization of its molecular characteristics, we determined whether this lipid A is contaminated with dihydroceramide lipids as described below.

**MALDI-TOF analysis of *P. gingivalis* lipid A.** The nonphosphorylated lipid A species monitored by MALDI-TOF MS revealed four abundant positive-ion lipid A species (*m/z* 1,406, 1,392, 1,378, and 1,364) and numerous lower-mass ions of lesser abundance, as show in Fig. 2B. Seven distinct nonphosphorylated lipid A species were identified in the LPS extract of *P. gingivalis*. All molecular species differed in mass by increments of 14 amu. MALDI-MS also revealed other positive ions of lower mass (*m/z* 1,050 to 1,190), and the origin of these lower-mass positive ions was evaluated using MALDI-MS/MS, with ion fragmentation evaluated by postsource decay. As shown in Fig. 3, the four dominant lipid A species listed above produced daughter (product) ions that predict loss of fatty acid constituents, as listed in Table 1. For example, the most abundant nonphosphorylated lipid A species of *P. gingivalis* (*m/z* 1,392 ion recovered as a sodium adduct) generated the dominant product ions depicted in Fig. 4B, C, and D as it undergoes postsource decay by MALDI-MS/MS. Other possible fragments of this precursor ion are shown in Table 1, depending on the R2 fatty acid substitutions of this lipid A. The other nonphosphorylated lipid A species of *P. gingivalis* are listed in Table 1 by precursor (parent) ion mass and by loss of specific fatty acid constituents (refer to Fig. 4 for the scheme of the lipid A fragmentation). Therefore, this analysis confirmed the fatty acid substitution characteristics of nonphosphorylated lipid A species of *P. gingivalis* but in greater detail than has been previously reported. Furthermore, it is postulated that the seven nonphosphorylated lipid A species should serve as substrate molecules for lipid A phosphorylation, resulting in at least seven monophosphorylated lipid A species and additional diphosphorylated species.

We attempted to analyze the phosphorylated lipid A species of *P. gingivalis* using MALDI-MS. The negative-ion species recovered using this approach (Fig. 2A) were virtually identical to those reported by Kumada et al. (23) using liquid secondary ion (LSI)-MS for detection of negative ions of *P. gingivalis* lipid A species. Using MALDI-MS, we identified ions consistent with penta-acylated, monophosphorylated lipid A species (*m/z* 1,702, 1,688, 1,674, 1,662, and 1,648), a tetra-acylated, diphosphorylated lipid A species (*m/z* 1,530), and tetra-acylated, monophosphorylated lipid A species (*m/z* 1,462, 1,448, 1,434, 1,420, and 1,406). However, because the lipid A negative ions were recovered in low abundances relative to the nonphosphorylated lipid A species, it was not possible to perform MALDI-MS/MS analysis of these lipid A negative ions. We evaluated lipid A by MALDI-MS in an amount that was 50- to 100-fold less concentrated than that reported previously (5). We observed strong positive-ion production, but only very limited negative-ion production at this con-

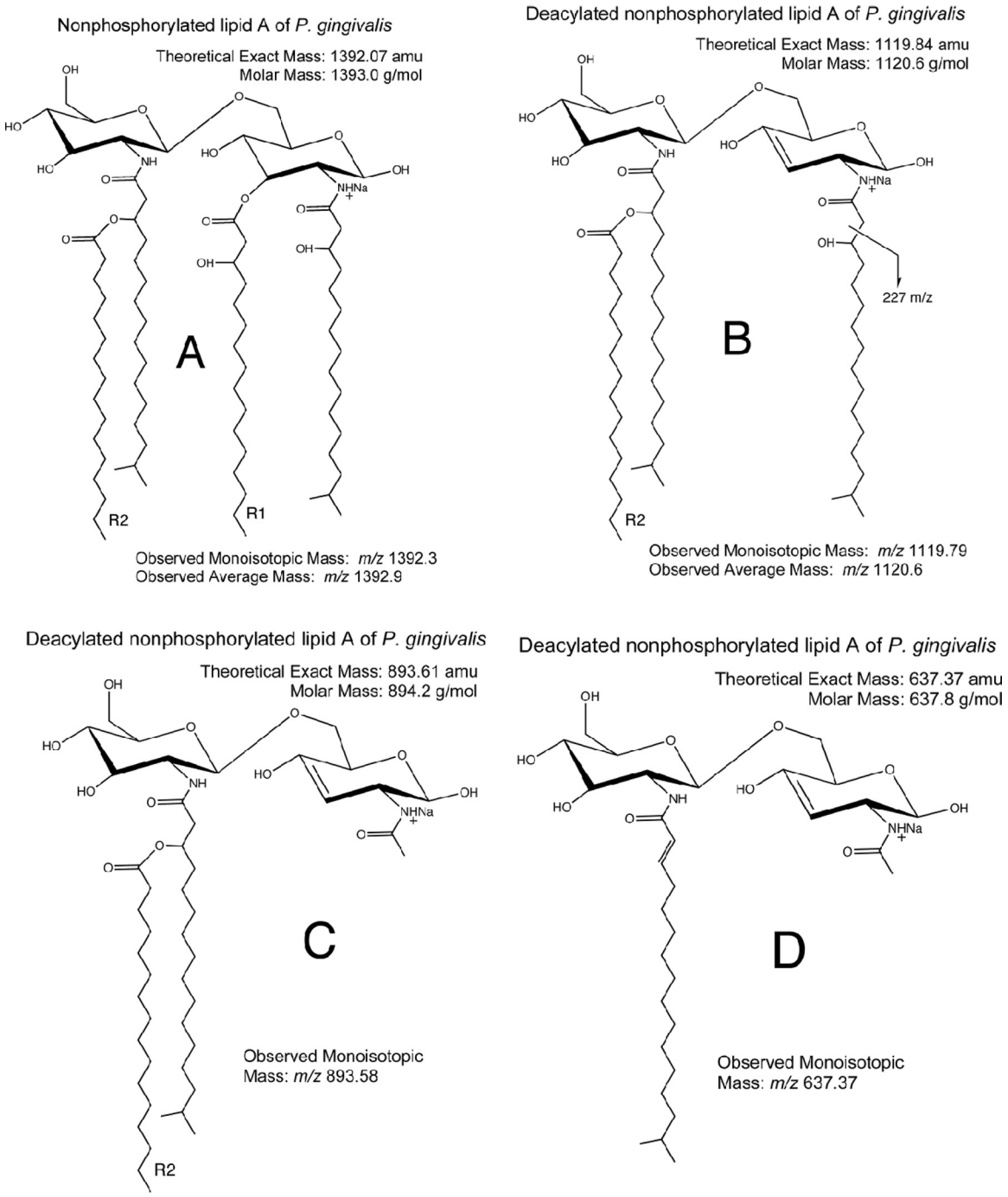


**FIG 4** Structural reconciliation of the dominant nonphosphorylated lipid A of *P. gingivalis*. Nonphosphorylated lipid A species are always detected as sodium adducts. (A) Shown is the structure of the most abundant lipid A positive ion (*m/z* 1,392.3). The observed monoisotopic ion mass was based on the TOF-generated mass spectrum (Fig. 2B), whereas the observed average mass is based on the quadrupole-generated mass spectrum (Fig. 5B). Deacylation of the *m/z* 1,392 lipid A (A) resulting from postsource decay yields a positive ion (B). (C and D) The positive ions show additional ion fragmentation for the *m/z* 1,392 positive ion. Similar fragmentation is observed with MALDI-MS/MS of the *m/z* 1,364, 1,378, and 1,406 ions (Fig. 3), and these fragments are used to generate the structural reconciliations shown in this figure. Refer to Table 1 for the predicted fatty acid substitutions for these nonphosphorylated lipid A species.

centration of lipid A, suggesting that phosphorylated lipid A species do not ionize as readily using this matrix and MALDI-MS. We did not attempt to maximize negative-ion recoveries either by modifying the matrix/lipid A ratio or by supplementing the matrix with other ion-enhancing agents, as reported by others (19, 45, 48). These issues will be addressed in future work.

**ESI-MS analysis of *P. gingivalis* lipid A.** Next, we analyzed the same *P. gingivalis* lipid A preparation using negative-ion ESI-MS to detect phosphorylated lipid A species (Fig. 5A). We observed high-mass ions (*m/z* 1,690, 1,676, 1,662, 1,648, 1,634, 1,620, 1,606, and 1,592), suggesting the presence of additional lipid A species beyond those previously observed using

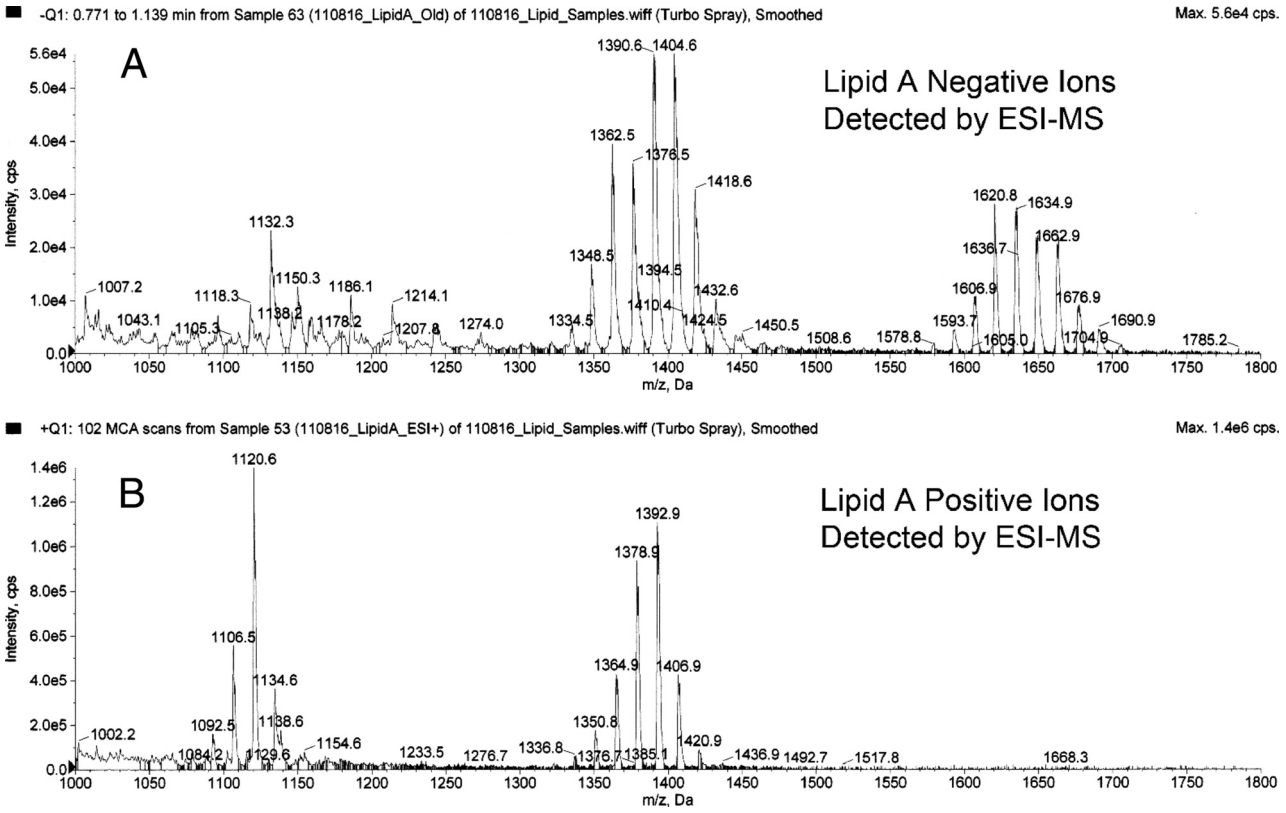


**FIG 5** Negative and positive ions of lipid A detected by ESI-MS. (A) Shown is the negative-ion spectrum of *P. gingivalis* lipid A, as demonstrated by ESI-MS. This analysis revealed a substantially different mass spectrum compared with MALDI-MS shown in Fig. 2A. (B) Shown is the positive-ion mass spectrum of lipid A obtained by ESI-MS. The lipid A positive ions are depicted as average ion masses and are consistent with the monoisotopic masses generated with MALDI-MS shown in Fig. 2B.

MALDI-MS. More importantly, we also observed a series of negative ions (*m/z* 1,432, 1,418, 1,404, 1,390, 1,376, 1,362, and 1,348) that have not been reported previously by MALDI-MS. We further evaluated the relationship between these higher- and lower-mass ions by using ESI-MS/MS. The generation of these lower-mass ions (*m/z* 1,432 to 1,348) could not be optimized by adjusting collision energy or gas pressure parameters, suggesting that they were not produced through a collision-induced dissociation of the higher-mass lipid A ions (*m/z* 1,690 to 1,592) but rather resulted from electrolytic de-esterification occurring in the ion source region of the instrument. We propose the following fragmentation scheme: the *m/z* 1,690 precursor ion generates predominantly the *m/z* 1,418 product ion through a process of de-esterification of the R1 fatty acid together with desaturation of the 3-4 saccharide bond (Fig. 1A and B). This lipid A fragmentation scheme has been previously described by others (25, 41). Additional product ions are generated from the *m/z* 1,690 precursor ion depending on the fatty acid constituent substituted in the R1 position (Table 2). Using this fragmentation scheme and the fatty acid constituents identified in this lipid A preparation, we can account for essentially all product ions resulting from the de-esterification at the R1 position of the monophosphorylated lipid A species of *P. gingivalis* (Table 2). ESI-MS/MS analysis of the most abundant de-esterified lipid A negative ions (*m/z* 1,418, 1,404, 1,390, and 1,376) revealed product ions, as depicted in Fig. 6. These product ions are consistent with the fragmentation of the phosphor-

**TABLE 2** Phosphorylated lipid A species of *P. gingivalis*[a]

| Precursor ion | First deacylated ion mass | Fatty acid leaving group (R1) |
|---|---|---|
| *m/z* 1,620 | *m/z* 1,376 | 3-OH $C_{14:0}$ |
| | *m/z* 1,362 | 3-OH iso $C_{15:0}$ |
| *m/z* 1,634 | *m/z* 1,390 | 3-OH $C_{14:0}$ |
| | *m/z* 1,376 | 3-OH iso $C_{15:0}$ |
| | *m/z* 1,362 | 3-OH $C_{16:0}$ |
| *m/z* 1,648 | *m/z* 1,390 | 3-OH iso $C_{15:0}$ |
| | *m/z* 1,376 | 3-OH $C_{16:0}$ |
| | *m/z* 1,362 | 3-OH iso $C_{17::0}$ |
| *m/z* 1,662 | *m/z* 1,404 | 3-OH iso $C_{15:0}$ |
| | *m/z* 1,390 | 3-OH $C_{16:0}$ |
| | *m/z* 1,376 | 3-OH iso $C_{17::0}$ |
| *m/z* 1,676 | *m/z* 1,418 | 3-OH iso $C_{15:0}$ |
| | *m/z* 1,404 | 3-OH $C_{16:0}$ |
| | *m/z* 1,390 | 3-OH iso $C_{17:0}$ |
| *m/z* 1,690 | *m/z* 1,432 | 3-OH iso $C_{15:0}$ |
| | *m/z* 1,418[b] | 3-OH $C_{16:0}$ |
| | *m/z* 1,404 | 3-OH iso $C_{17:0}$ |

[a] The lipid A preparation of *P. gingivalis* was subjected to electrospray-MS/MS, as described in Materials and Methods. Lipid A was dissolved in hexane-isopropanol-water, 6:8:0.75 (vol/vol/vol), at a concentration of approximately 0.5 $\mu$g/$\mu$l, and this solution was infused at a rate of 20 $\mu$l/min. Each precursor ion generates the indicated deacylated ions when the listed fatty acid is lost from the R1 position (Fig. 1). Though the fatty acid lost from the R1 position shown in Fig. 1 is 3-OH $C_{16:0}$, other fatty acids can substitute in the R1 position as listed.
[b] See Fig. 1B.

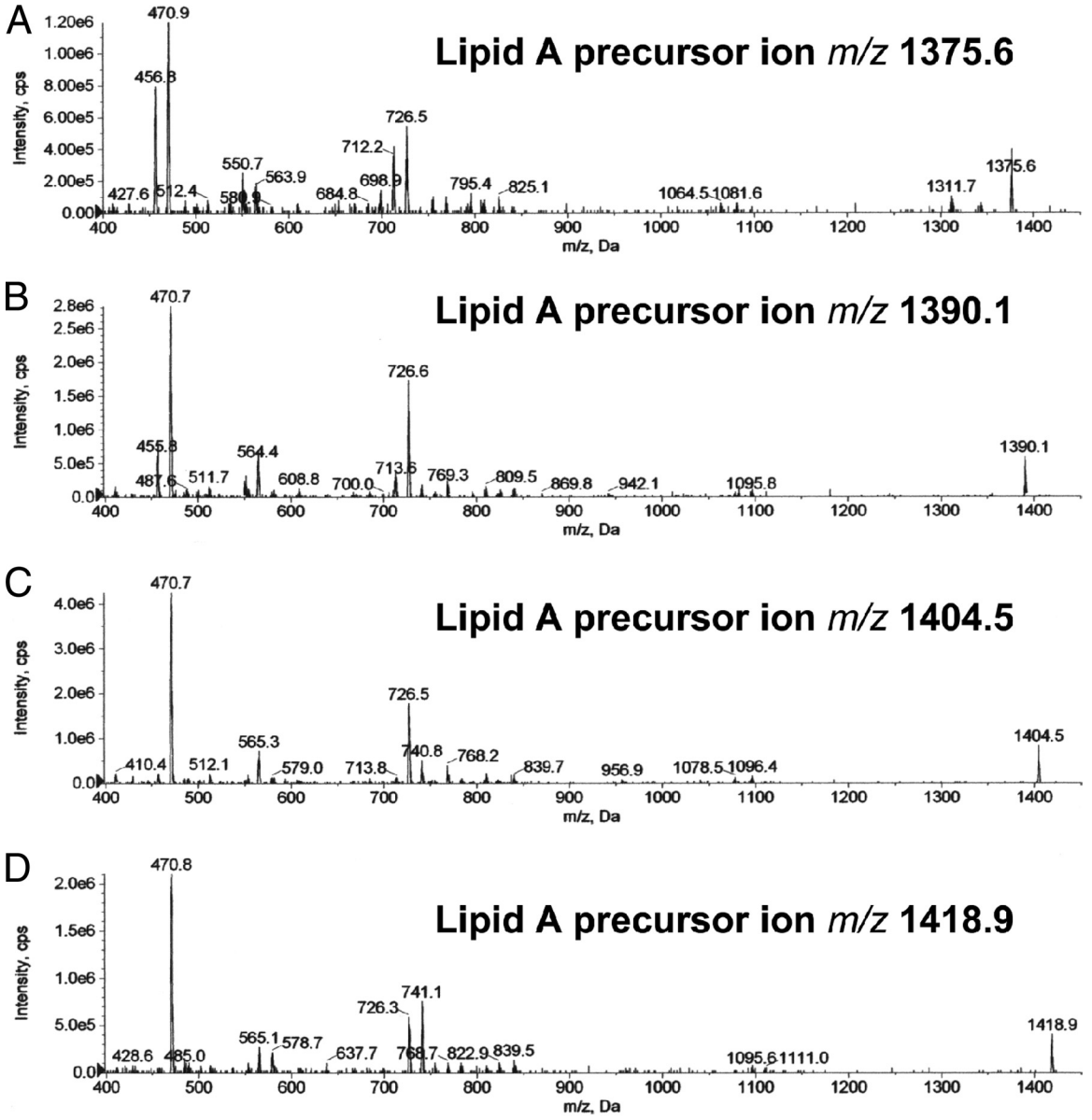


**FIG 6** ESI-MS/MS of dominant phosphorylated lipid A species (negative ions). The dominant phosphorylated lipid A species (*m/z* 1,418, 1,404, 1,390, and 1,376) generated through post-ion source de-esterification and desaturation (Fig. 1A and B) were evaluated for characteristic product ions resulting from collision induced dissociation. The product ions produced from these precursor ions are depicted for the mass range *m/z* 400 to 1,500. (D) The ESI-MS/MS spectrum for the *m/z* 1,418 monophosphorylated lipid A ion shown was used to reconcile the loss of fatty acids, as proposed in Fig. 1. Loss of fatty acids from the remaining lipid A species (A to C) are reconciled in Tables 2 and 3.

ylated lipid A species summarized in Table 3. As an example, Fig. 1 depicts the fragmentation of the *m/z* 1,418 precursor ion (Fig. 1B to E). This fragmentation scheme can be applied to other phosphorylated lipid A precursor ions as well. Although the distribution of high-mass phosphorylated lipid A ions differs between the MALDI-MS and ESI-MS approaches, the number of monophosphorylated lipid A species identified by ESI-MS is consistent with the number of nonphosphorylated lipid A species identified by either MALDI-MS or ESI-MS. Furthermore, our results also suggest that recovery of phosphorylated lipid A species can be monitored in biological samples using electrospray-MS/MS transitions, as will be subsequently demonstrated.

Next, we analyzed the same *P. gingivalis* lipid A preparation using ESI-MS to detect nonphosphorylated lipid A species (Fig. 5B). The positive ions observed were essentially identical to those observed by positive-ion MALDI-MS, as shown in Fig. 2B. The precursor-product ion transitions for the dominant positive lipid A ions, as determined by ESI-MS/MS (data not shown), revealed mass spectra essentially identical to those depicted in Fig. 3. Therefore, the MALDI-MS and ESI-MS analyses of nonphosphorylated lipid A species provide essentially identical recovery of positive molecular ions and ion fragments.

**Recovery of *P. gingivalis* lipid A and phosphorylated dihydroceramides in dental samples.** Next, we evaluated lipid extracts from calculus-contaminated teeth, impacted third molars, and

**TABLE 3** Phosphorylated lipid A species of *P. gingivalis*[a]

| Precursor ion[c] | Lipid A fragment[d] | Fatty acid leaving group (R3) | Lipid A fragment[e] | Fatty acid leaving group (R2) |
|---|---|---|---|---|
| *m/z* 1,375 | *m/z* 727[b] | $C_{16:0}$ | *m/z* 565 | $C_{16:0}$ |
| | *m/z* 713 | Iso $C_{15:0}$ | *m/z* 551[b] | Iso $C_{15:0}$ |
| | *m/z* 698 | $C_{14:0}$ | *m/z* 537 | $C_{14:0}$ |
| *m/z* 1,389 | *m/z* 727[b] | $C_{16:0}$ | *m/z* 565[b] | $C_{16:0}$ |
| | *m/z* 713 | Iso $C_{15:0}$ | *m/z* 551 | Iso $C_{15:0}$ |
| *m/z* 1,403 | *m/z* 741 | Iso $C_{17:0}$ | *m/z* 579 | Iso $C_{17:0}$ |
| | *m/z* 727[b] | $C_{16:0}$ | *m/z* 565[b] | $C_{16:0}$ |
| | *m/z* 713 | Iso $C_{15:0}$ | | |
| *m/z* 1,417 | *m/z* 741[b] | Iso $C_{17:0}$ | *m/z* 579[b] | Iso $C_{17:0}$ |
| | *m/z* 727 | $C_{16:0}$ | *m/z* 565 | $C_{16:0}$ |

[a] The lipid A preparation of *P. gingivalis* was subjected to ESI-MS/MS, as described in Materials and Methods. Lipid A was dissolved in hexane-isopropanol-water, 6:8:0.75 (vol/vol/vol), at a concentration of approximately 0.5 μg/μl, and this solution was infused at a rate of 20 μl/min. Each precursor ion generates the indicated deacylated ions when the listed fatty acids are first deacylated from the R2 position (Fig. 1) and subsequently deacylated from the R3 position. The fatty acids listed in Table 1 were shown by sodium methoxide treatment and GC-MS analysis to be ester linked in this lipid A preparation. Additional phosphorylated lipid A species appear as negative ions, with masses of *m/z* 1,360, 1,430, and 1,444 (Fig. 5). However, these additional lipid A species were recovered in lower-ion abundances, and ESI-MS/MS analysis was not feasible.

[b] Dominant ion transitions noted with MS/MS transitions.

[c] See Fig. 1B.

[d] See Fig. 1C.

[e] See Fig. 1E.

subgingival plaque samples for the presence of lipid A species. Subgingival plaque samples from chronic periodontitis sites represent disease-related biofilm samples. For this analysis, we used both single-stage MS detection and MRM-MS detection of ion transitions specific for the lipid A species noted above. By MALDI-MS analysis, lipid extracts from calculus-contaminated teeth and subgingival plaque samples did not reveal either the positive or negative lipid A molecular ions described above (data not shown) or diphosphorylated lipid A species previously reported by others (5, 8, 11). For MRM-MS analysis, ion transitions were used to quantify the most abundant lipid A negative ions described above. For quantification of lipid A species, we monitored the following MRM-negative ion transitions: *m/z* 1,418 to 740, *m/z* 1,418 to 579, *m/z* 1,404 to 726 (panel C), *m/z* 1,404 to 565 (panel D), *m/z* 1,390 to 712 (panel A), and *m/z* 1,390 to 551 (panel B) (only the *m/z* 1,404 and 1,390 transitions are depicted in Fig. 7 through 10). As a comparison, MRM transitions indicating high- and low-mass phosphoglycerol dihydroceramides (PG DHC; *m/z* 960 to 171 and *m/z* 932 to 171, respectively) or high- and low-mass phosphoethanolamine dihydroceramides (PE DHC; *m/z* 705 to 140 and *m/z* 677 to 140, respectively) (33) were evaluated in parallel with the assessment of lipid A ion transitions in the lipid extracts of these dental samples. Our results showed that negligible levels of phosphorylated lipid A ions are recovered in lipid extracts of teeth with subgingival calculus ($n = 2$) (Fig. 7). The recovery of phosphorylated lipid A species versus phosphorylated dihydroceramides are shown in Fig. 7, left and right, respectively. Note that the free lipid A preparation of *P. gingivalis* was injected as a positive control after the individual lipid extracts of teeth were infused (Fig. 7, left). The ion transitions characteristic for free lipid A species are clearly evident with the lipid A standard but are not present in the lipid extracts of teeth. The phosphorylated dihydroceramide ion abundances in tooth lipid extracts were at least 1,000 to 10,000 times greater than those in the lipid A ion traces. Similar results were observed for subgingival plaque samples (Fig. 8), although the differences in ion abundances between the lipid A and dihydroceramide lipid scans were not as large as those observed with lipid extracts from teeth. Regardless, the levels of free lipid A in these dental samples are negligible compared with the levels of phosphorylated dihydroceramide lipids. Lipid extracts from impacted third molars contained negligible levels of phosphoethanolamine dihydroceramides and lipid A species, with very low levels of phosphoglycerol dihydroceramide lipids detected. Our previous studies indicated that hydrolysis of plaque or gingival tissue lipid extracts yields substantial levels of 3-OH iso $C_{17:0}$, which could reflect the presence of bacterial lipids, including dihydroceramide lipids or free lipid A species. We now conclude that 3-OH iso $C_{17:0}$ previously recovered from lipid extracts of diseased dental samples (26, 29) does not reflect the presence of phosphorylated lipid A of *P. gingivalis*.

More importantly, we examined the free lipid A preparation of *P. gingivalis* LPS for contamination with phosphorylated dihydroceramides using single-stage MS and MRM-MS analysis. By single-stage MS analysis, we observed significant levels of the characteristic molecular ions of substituted phosphoglycerol dihydroceramides (*m/z* 960, 946, and 932) and molecular ions of phosphoethanolamine dihydroceramides (*m/z* 705, 691, and 677) (31) in two independent lipid A preparations isolated from *P. gingivalis* LPS (data not shown). Furthermore, we observed characteristic MRM-MS ion transitions that indicate significant levels of phosphorylated dihydroceramide lipids in lipid A extracts of *P. gingivalis* (Fig. 10). Therefore, we now provide evidence that lipid A derived from LPS of *P. gingivalis* prepared by the Tri-Reagent method (46) is contaminated with phosphorylated dihydroceramides of *P. gingivalis*.

## DISCUSSION

This investigation is, in part, directed toward a reassessment of the role of *P. gingivalis* virulence factors in promoting inflammatory and tissue-destructive processes associated with periodontal diseases. This reassessment comes at a time when emerging evidence implicates non-LPS virulence factors of *P. gingivalis*, including phosphorylated dihydroceramide lipids, as major contributing factors to the pathogenesis of chronic destructive periodontal disease (31, 33, 43). There is concern that the LPS of *P. gingivalis* is not critical in promoting destructive periodontal diseases because the levels of LPS from *P. gingivalis* are negligible in diseased gingival tissues from chronic periodontitis sites (26, 30). The lack of LPS of *P. gingivalis* in diseased gingival tissues also suggests that *P. gingivalis* invasion is not prominent in diseased periodontal tissues. In the absence of significant bacterial invasion, putative virulence factors should be recovered in diseased tissues at levels capable of promoting inflammatory or tissue-destructive processes. Surprisingly, few virulence factors of *P. gingivalis* or any other periodontal pathogen have met this fundamental criterion for implication in the pathogenesis of periodontal disease. It was the application of this concept that led to the discovery of *P. gingivalis* dihydroceramide lipids in diseased periodontal tissues, while little if any LPS from this organism could be identified in the

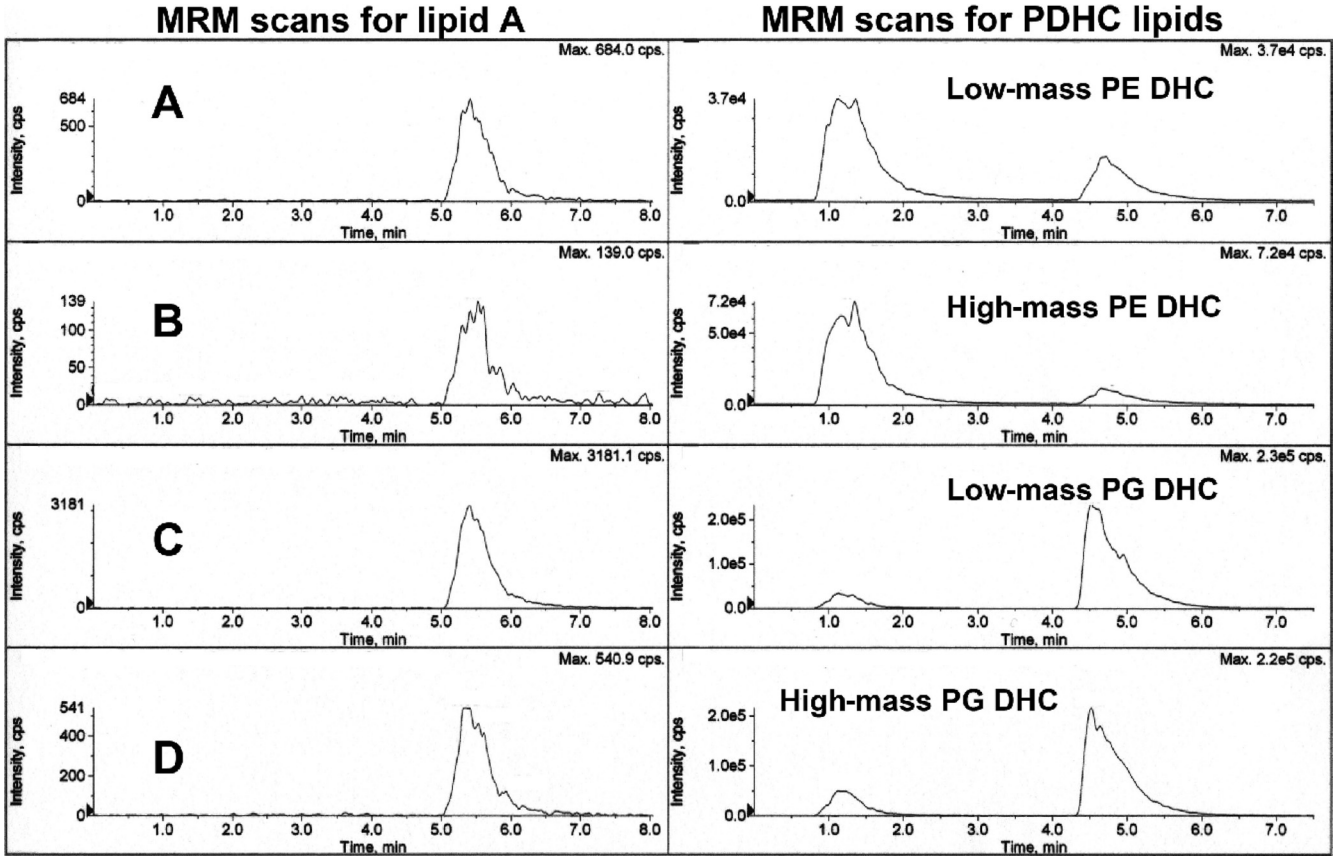


**FIG 7** Recovery of phosphorylated lipid A species and phosphorylated dihydroceramide (PDHC) lipids in organic solvent extracts from calculus-contaminated teeth. Teeth extracted from two patients were individually pooled and extracted for lipids, as described in Materials and Methods. A sample of each lipid extract was evaluated for phosphorylated lipid A species using MRM-MS quantification of transitions characteristic for the dominant phosphorylated lipid A species detected in Fig. 5 (*m/z* 1,404 and 1,390 precursor ions were evaluated). (Left) Shown are the MRM-MS profiles for the *m/z* 1,390 to 726 (A), 1,390 to 565 (B), 1,404 to 726 (C), and 1,404 to 565 (D) ion transitions. The MS/MS transitions characteristic for the *m/z* 1,418 lipid A precursor ion were also evaluated and confirmed negligible levels of this lipid A in lipid extracts from diseased teeth (data not shown). The tooth lipid extracts (5 $\mu$g each) were injected at 1 and 3 min. A sample of *P. gingivalis* lipid A was injected at 4.5 min. In a separate analysis, we evaluated the same tooth lipid extracts for characteristic phosphorylated dihydroceramide lipids using MRM-MS analysis and previously characterized mass spectrometric parameters for these lipid products. Tooth lipid samples (5 $\mu$g each) were injected at 1 and 3.5 min. The phosphorylated dihydroceramide lipids elute in the following order from top to bottom: low-mass PE DHC lipid (*m/z* 677 to 140 negative-ion transition), high-mass PE DHC lipid (*m/z* 705 to 140 negative-ion transition), low-mass PG DHC lipid (*m/z* 932 to 171 negative-ion mass), high-mass PG DHC lipid (*m/z* 960 to 171 negative-ion mass) (31, 33). Note that the ion abundances for phosphorylated dihydroceramides are 3 or 4 orders of magnitude greater than the MS scan abundances for lipid A species.

same tissue samples (26, 30). Despite continued research emphasis on *P. gingivalis* lipid A and LPS constituents in promoting inflammatory and tissue-destructive processes in periodontal diseases, little evidence has been forthcoming to demonstrate the presence of lipid A or LPS in diseased periodontal tissues. In addition, other virulence factors of *P. gingivalis* proposed to contribute to the expression of periodontal disease, including fimbriae, have not been demonstrated in diseased periodontal tissues. Therefore, our evidence argues strongly for more intensive investigation of *P. gingivalis* virulence factors, such as phosphorylated dihydroceramides, that are both plentiful in destructive periodontal disease sites and are established to engage relevant host innate immune systems (TLR2).

In order to determine whether free lipid A accounts for 3-OH iso $C_{17:0}$ detected in lipid extracts of diseased teeth and subgingival plaque samples (26, 30), it was first necessary to characterize both positive- and negative-ion forms of lipid A purified from *P. gingivalis* (ATCC 33277). Using positive-ion MALDI-MS, we show that the type strain of *P. gingivalis* contains the same nonphosphorylated lipid A ions that were recently reported for the 1626 KO strain of *P. gingivalis* (8). Our results suggest the following: either the nonphosphorylated lipid A species form positive ions more efficiently with MALDI-MS or these nonphosphorylated lipid A species are far more plentiful in the LPS of *P. gingivalis* than the phosphorylated lipid A species, consistent with a previous report by Coats et al. (8). Given the apparent levels of nonphosphorylated lipid A species present in *P. gingivalis* LPS isolates, it seems reasonable that LPS-containing nonphosphorylated lipid A species should be separated from LPS-containing phosphorylated lipid A species before these structurally distinct LPS isolates are evaluated for biological effects.

Regarding the structural reconciliation of *P. gingivalis* lipid A species, our results indicate that the ionization mode used to characterize phosphorylated lipid A species of *P. gingivalis* has a major effect on the types of species identified and the relative amounts of these species. MALDI-MS showed only five negative ions for

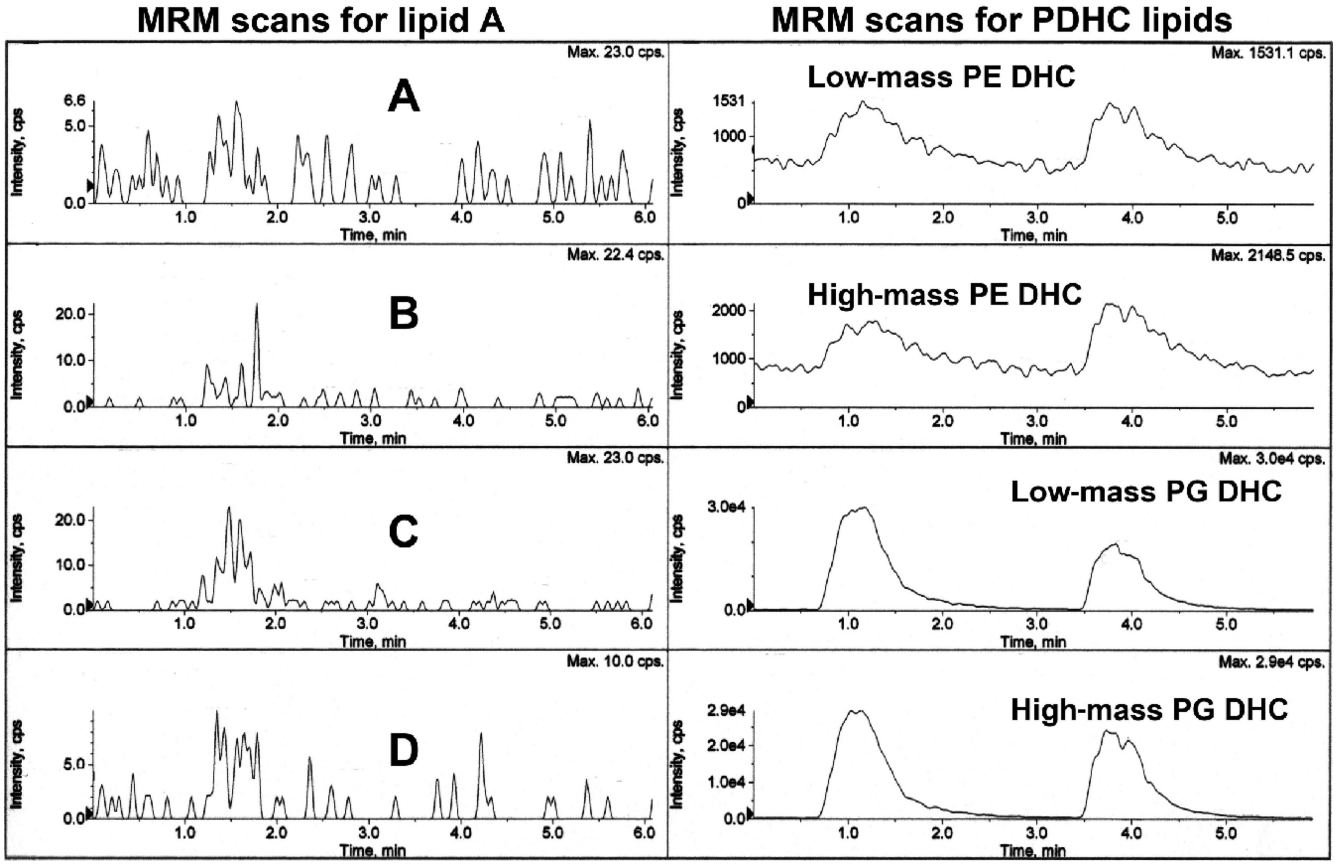


**FIG 8** Recovery of phosphorylated lipid A species and phosphorylated dihydroceramide lipids in organic solvent extracts from subgingival plaque samples. Subgingival plaque samples were collected, pooled by individual, and extracted for lipids, as described in Materials and Methods. A sample of each lipid extract was evaluated for phosphorylated lipid A species (left) and for phosphorylated dihydroceramide lipids (right) using the same order of ion transition monitoring and instrument parameters as shown in Fig. 7. Lipid samples were injected at 5 s and 2.5 min. Note that the phosphorylated dihydroceramide lipids show at least 2 or 3 orders of magnitude greater abundance compared with the phosphorylated lipid A species in the same lipid extracts of subgingival plaque samples.

penta-acylated, monophosphorylated lipid A species, yet positive-ion MALDI-MS shows at least seven nonphosphorylated lipid A species. Furthermore, negative-ion MALDI-MS revealed five tetra-acylated, monophosphorylated lipid A species along with the penta-acylated, monophosphorylated lipid A species. In contrast, ESI-MS of the same lipid A preparation showed seven penta-acylated, monophosphorylated lipid A species and seven monophosphorylated, tetra-acylated lipid A species resulting from deacylation of the R1 fatty acid and desaturation in the 3-4 saccharide bond (Fig. 1A and B). Therefore, the number of phosphorylated lipid A species recovered by ESI-MS is consistent with the number of nonphosphorylated lipid A species detected by either MALDI-MS or ESI-MS. Furthermore, ESI-MS (Fig. 5A) did not detect tetra-acylated, monophosphorylated lipid A species shown in the MALDI-MS scan (Fig. 2A), suggesting that the MALDI-MS ionization process actually produces lipid A ions that are de-esterified in the 3′ position without concurrent desaturation. Taken together, this evidence indicates that monophosphorylated, penta-acylated lipid A species can fragment to tetra-acylated, monophosphorylated lipid A species by MALDI-MS, whereas ESI-MS causes fragmentation to tetra-acylated, monophosphorylated lipid A species that are de-esterified in the R1 fatty acid and desaturated in the 3-4 saccharide bond (Fig. 4). This evidence suggests that reliance on a single ionization approach does not provide sufficient information to accurately reconcile phosphorylated lipid A structures in complex mixtures.

According to a recent report by Coats et al. (8), using MALDI-MS/MS, monophosphorylated lipid A species of *P. gingivalis* retain the phosphate group in the 4′ position rather than the 1 saccharide position (Fig. 1). However, based on the known fatty acid substitutions that occur in the R2 and R3 positions described here for the negative-ion lipid A species, each of the higher-mass $A_2$ ion fragments described by Coats et al. (8) should be recovered in our relevant lipid A fragments for the differing lipid A precursor ions. Using ESI-MS/MS, we did not observe $A_2$ ion fragments that are consistent with phosphate substitution of lipid A in the 4′ position. Because the $A_2$ ions described by Coats et al. (8) were recovered in low abundances, another possibility is that these investigators isolated lipid A with phosphate substitution in either the 1 position or 4′ position of lipid A, but the 1 position phosphate substitution is the dominant form (23). ESI-MS/MS analysis of *m/z* 1,676, 1,662, 1,648, and 1,634 negative-ion species (Fig. 5) of *P. gingivalis* lipid A failed to identify ion fragments consistent with a 4′ phosphate substitution of lipid A, as reported by Coats et al. (8). Our structural reconciliation of the location of the phosphate group in monophosphorylated lipid A species is therefore consistent with that reported by Kumada et al. (23).

Because the previously reported recovery of 3-OH iso $C_{17:0}$ in

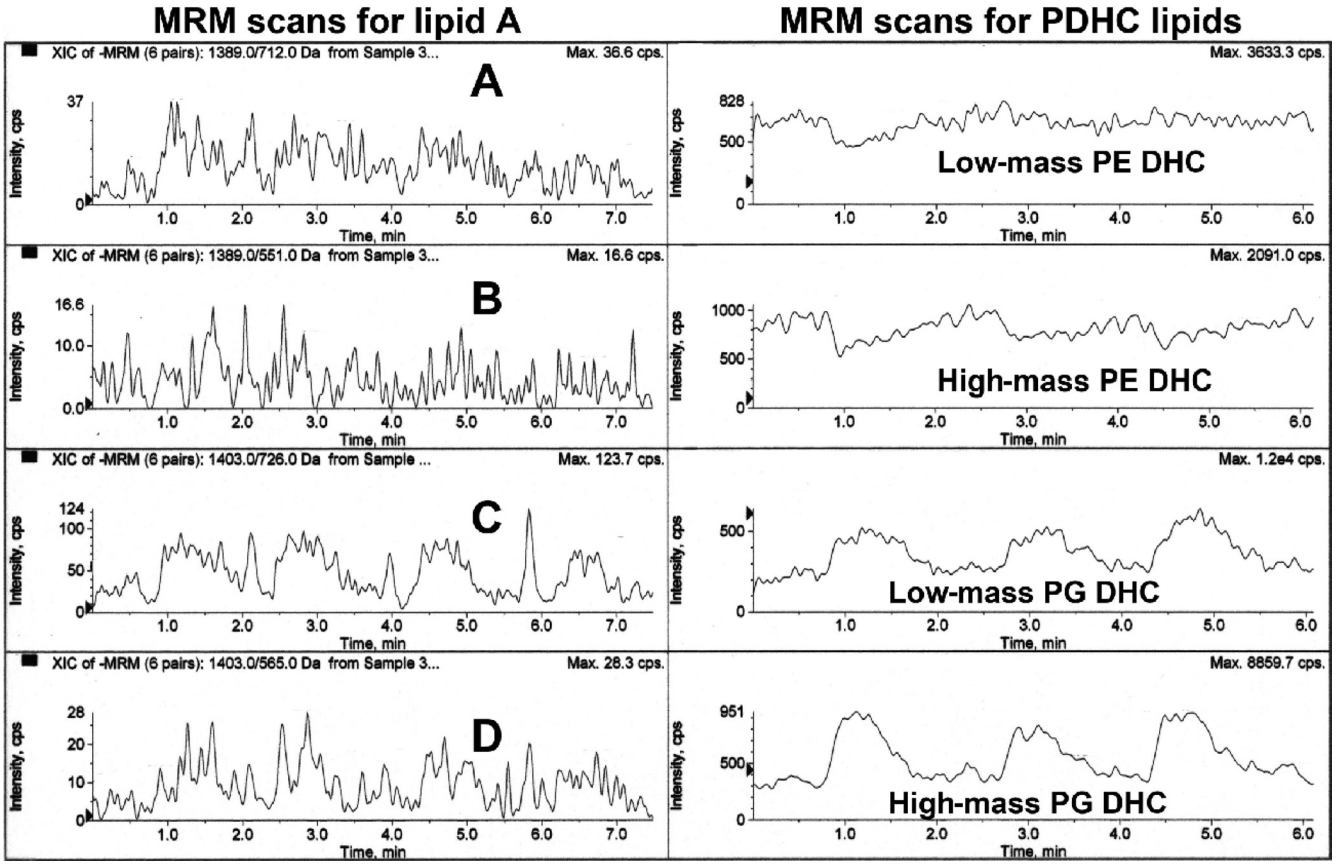


**FIG 9** Recovery of phosphorylated lipid A species and phosphorylated dihydroceramide lipids in lipid extracts from impacted third molars. Impacted third molars collected from three patients were individually extracted for lipids, as described in Materials and Methods. A sample of each lipid extract (5 $\mu$g) was evaluated for phosphorylated lipid A species (left) and for phosphorylated dihydroceramide lipids (right) using the same order of ion transition monitoring and instrument parameters as shown in Fig. 7. Individual tooth samples were injected at 5 s, 2 min, and 3.5 min. Note that only the phosphoglycerol dihydroceramide (PG DHC) lipids were detected, but the ion abundances were at least 3 orders of magnitude less than those observed with an equivalent amount of lipid extract from calculus-contaminated teeth. Phosphoethanolamine dihydroceramides and phosphorylated lipid A species were not detected in these samples.

organic extracts of subgingival plaque and diseased gingival tissues (26, 30) could reflect the presence of free lipid A of *P. gingivalis*, the recovery of free lipid A species was evaluated in lipid extracts of calculus-contaminated teeth, impacted third molars, and subgingival plaque samples. Lipid A was evaluated in these dental samples as phosphorylated species quantified by ESI-MRM-MS. As a comparison, we evaluated replicate samples of each dental extract for phosphorylated dihydroceramide lipids of *P. gingivalis* (33). Quantification of lipid A species and phosphorylated dihydroceramide lipids utilized MRM-MS with optimized ion transitions recorded for the high- and low-mass substituted phosphoglycerol dihydroceramide (PG DHC) and phosphoethanolamine dihydroceramide (PE DHC) lipids (31) as well as the *m/z* 1,403 to 726 or 565 and the *m/z* 1,389 to 712 or 551 transitions for the dominant phosphorylated lipid A species of *P. gingivalis*. Figure 7 shows the MRM-MS scans indicating high- and low-mass PG DHC and PE DHC lipids in extracts from calculus-contaminated teeth removed from two different individuals. One tooth lipid extract eluted with peak recovery of phosphorylated dihydroceramide (PDHC) lipids at 1.3 min, and the second eluted with peak PDHC recovery at 3.8 min. The same tooth lipid extracts were then evaluated for the two dominant phosphorylated lipid A species produced by *P. gingivalis* (Fig. 7A through D). MRM-MS of the tooth samples revealed no lipid A negative ions at the elution times for PDHC lipids. As a comparison, the lipid A preparation of *P. gingivalis* was injected as a positive control, and peak negative-ion recovery for all scans was noted at about 5.4 min. The lipid extracts from calculus-contaminated teeth contained substantial levels of phosphorylated dihydroceramide lipids but negligible levels of lipid A from *P. gingivalis*. Analysis of lipid extracts from subgingival plaque samples ($n = 2$) revealed significant levels of phosphorylated dihydroceramide lipids with negligible levels of *P. gingivalis* lipid A species (Fig. 8). However, lipid extracts from impacted third molars contained negligible levels of lipid A and phosphoethanolamine dihydroceramide lipids, with very small amounts of phosphoglycerol dihydroceramide lipids observed. In summary, the levels of monophosphorylated lipid A species in all dental samples from periodontitis disease sites were negligible compared with the phosphorylated dihydroceramide lipids. Therefore, the previously reported recovery of 3-OH iso $C_{17:0}$ in lipid extracts of diseased teeth and subgingival plaque (26, 29) does not result from the presence of free lipid A species.

The Tri-Reagent method was previously shown to extract LPS constituents from *P. gingivalis* that contain diphosphorylated penta-acylated lipid A species as well as monophosphorylated tetra- and penta-acylated lipid A species, whereas the $MgCl_2$/

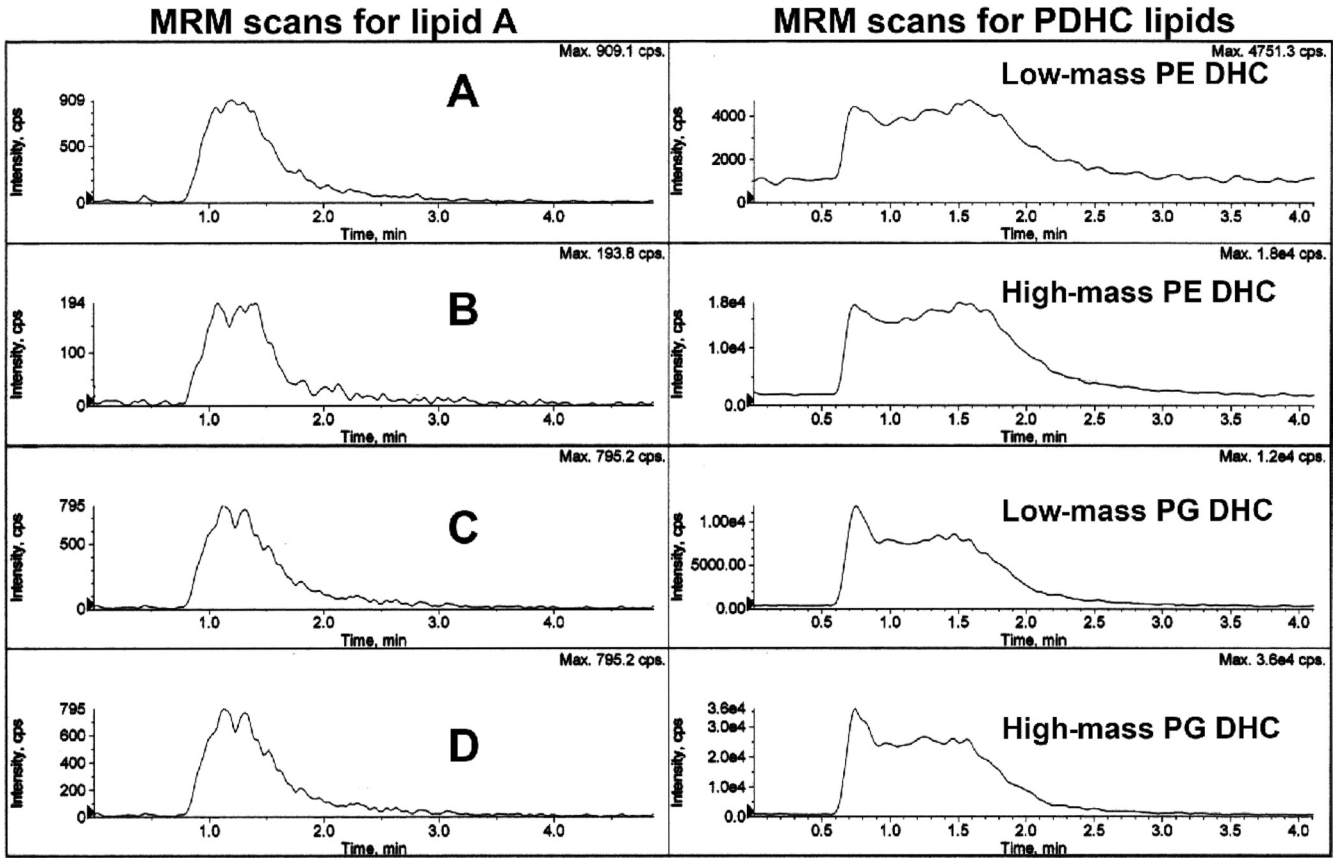


**FIG 10** Recovery of phosphorylated dihydroceramide lipids in the lipid A extract of *P. gingivalis*. Lipid A of *P. gingivalis* was prepared as described in Materials and Methods, and the lipid A was dissolved in hexane-isopropanol-water (6:8:0.75, vol/vol/vol) at 0.5 $\mu$g/$\mu$l. Lipid A (approximately 2 $\mu$g) was evaluated for characteristic ion transitions for the dominant phosphorylated lipid A species (left; using the same MRM-MS transitions as described in Fig. 7) and phosphorylated dihydroceramide lipids (right; using the same MRM-MS transitions as described in Fig. 7). Note that the abundances for the phosphorylated dihydroceramide lipids are higher than those for the phosphorylated lipid A species.

EtOH extraction method recovered LPS constituents from *P. gingivalis* that included only the monophosphorylated tetra-acylated species of lipid A (11). According to Yi and Hackett (46), Tri-Reagent extraction of LPS yields a lipid A preparation that contains considerably lower levels of contaminating substances compared with lipid A recovered with the phenol water extraction method of Westphal and Jann (44). Therefore, the Tri-Reagent method appears to be preferable to other LPS extraction methods because it provides the widest range of lipid A species with minimal non-LPS contaminants. In addition to the Tri-Reagent method, some investigators have included additional purification approaches for *P. gingivalis* LPS prior to hydrolysis and recovery of lipid A. These additional purification steps included either a Folch et al. (12) extraction (5, 11) or a Bligh and Dyer (6) extraction procedure (8) to remove contaminating phospholipids. However, removal of phospholipids was not verified by mass spectrometric methods in these studies. Our results clearly show that up to three successive Bligh and Dyer extractions of the Tri-Reagent-prepared LPS of *P. gingivalis* will recover significant levels of contaminating phosphorylated dihydroceramide lipids. This indicates that successive phospholipid extractions will only partially remove phosphorylated dihydroceramide lipids.

Relevant to the present studies is the recently observed capacity of specific *P. gingivalis* dihydroceramides (PE DHC) to engage TLR2 in activating dendritic cells and in promoting autoimmune disease in a murine model of multiple sclerosis (29). The effects of PE DHC lipids were reported to be comparable to the effects produced by lipoprotein (MMP, TLR2 ligand) (29). TLR2 dependence was demonstrated using a highly purified PE DHC lipid preparation that was free of protein, complex carbohydrate, or lipid A components of *P. gingivalis*, as demonstrated using structural nuclear magnetic resonance (NMR) studies and collisional mass spectrometry (31). The PE DHC lipids were shown to worsen experimental autoimmune encephalomyelitis (EAE) in wild-type mice using very low doses administered intraperitoneally, but EAE was not affected in TLR2 knockout mice by these lipids (29). Other coreceptors are likely to be involved in this TLR2 engagement (i.e., TLR1, TLR6, and perhaps others), but their roles remain to be characterized. Our recent work clearly shows that specific *P. gingivalis* dihydroceramide lipids engage TLR2 in promoting immune-regulated disease *in vivo* and immune cell activation *in vitro*.

The capacity of *P. gingivalis* LPS or its lipid A to engage TLR2 has been controversial for several reasons. Depending on the extraction method of *P. gingivalis* LPS, reports have shown conflicting evidence regarding cell activation through TLR2 (21, 22). Lipid A preparations of *P. gingivalis* have been reported to interact with TLR2 and/or TLR4 (11) or to interfere with TLR4 responses

(42). However, Ogawa et al. have synthesized the most abundant form of lipid A of *P. gingivalis* and demonstrated that this synthetic lipid A engages only TLR4 (35, 40). Conversely, this group has shown that a lipoprotein of *P. gingivalis* acts only through TLR2 and suggested that lipid A preparations of *P. gingivalis* isolated by others may be contaminated with lipoprotein (2, 35). A recent report demonstrated that synthetic lipid A of *P. gingivalis* activates cells only through TLR4, whereas LPS or the dominant form of lipid A extracted from *P. gingivalis* activates through TLR2 or TLR4, leading these authors to speculate that other bioactive contaminants account for the TLR2-mediated effects observed with *P. gingivalis* LPS isolates (24). Finally, TLR2-transfected cells exposed to *P. gingivalis* LPS respond with weaker cytokine secretory responses than the known TLR2 ligand, *Staphylococcus aureus* lipoteichoic acid (42). All together, this evidence raises significant concern that non-LPS contaminants may be largely responsible for the TLR2 activity attributed to *P. gingivalis* LPS. Furthermore, fimbriae of *P. gingivalis* (3, 17, 18) and BspA of *Tannerella forsythia* (16) are reported to engage TLR2. Since these substances are anchored in bacterial membranes and because *T. forsythia* synthesizes the same phosphorylated dihydroceramides as *P. gingivalis* (33), we suspect that fimbria and BspA preparations are also contaminated with bacterial lipids that contribute to their reported TLR2 activity.

In summary, our studies have further elucidated the structures of lipid A species of *P. gingivalis* using a combination of MALDI-MS/MS and ESI-MS/MS. Furthermore, ESI-MS/MS can be extended to include quantification of specific lipid A species within dental samples when MRM-MS is employed. However, using both of these mass spectrometric approaches, we could not detect free lipid A species of *P. gingivalis* in lipid extracts from either diseased teeth or subgingival plaque samples. In contrast, we observed significant amounts of phosphorylated dihydroceramides in these dental samples. Finally, LPS and lipid A preparations of *P. gingivalis* extracted by the Tri-Reagent method are contaminated with phosphorylated dihydroceramide lipids that are known to act through TLR2. This observation raises the possibility that the previously reported capacity of *P. gingivalis* and *P. gingivalis* LPS and lipid A to mediate biological functions via TLR2 may actually result, at least in part, from the presence of contaminating phosphorylated dihydroceramide lipids.

## ACKNOWLEDGMENTS

We thank Jean Kanyo of the Keck Biotechnology Research Laboratory of Yale University School of Medicine for her assistance with the MALDI-MS analyses.

This work was supported in part by National Multiple Sclerosis Society grant 4070-A-6 and by National Institutes of Health grant DE021055.

## REFERENCES

1. **Asai Y, et al.** 2005. Lipopolysaccharide preparation extracted from *Porphyromonas gingivalis* lipoprotein-deficient mutant shows a marked decrease in Toll-like receptor 2-mediated signaling. Infect. Immun. **73**: 2157–2163.
2. **Asai Y, Makimura Y, Ogawa T.** 2007. Toll-like receptor 2-mediated dendritic cell activation by a *Porphyromonas gingivalis* synthetic lipopeptide. J. Med. Microbiol. **56**:459–465.
3. **Asai Y, Ohyama Y, Gen K, Ogawa T.** 2001. Bacterial fimbriae and their peptides activate human gingival epithelial cells through Toll-like receptor 2. Infect. Immun. **69**:7387–7395.
4. **Bainbridge BW, Coats SR, Darveau RP.** 2002. *Porphyromonas gingivalis* lipopolysaccharide displays functionally diverse interactions with the innate host defense system. Ann. Periodontol. **7**:29–37.
5. **Berezow AB, et al.** 2009. The structurally similar, penta-acylated lipopolysaccharides of *Porphyromonas gingivalis* and Bacteroides elicit strikingly different innate immune responses. Microb. Pathog. **47**:68–77.
6. **Bligh EG, Dyer WJ.** 1959. A rapid method of total lipid extraction and purification. Can. J. Biochem. Physiol. **37**:911–917.
7. **Caroff M, Tacken A, Szabo L.** 1988. Detergent-accelerated hydrolysis of bacterial endotoxins and determination of the anomeric configuration of the glycosyl phosphate present in the "isolated lipid A" fragment of the *Bordetella pertussis* endotoxin. Carbohydr. Res. **175**:273–282.
8. **Coats SR, et al.** 2011. The lipid A phosphate position determines differential host Toll-like receptor 4 responses to phylogenetically related symbiotic and pathogenic bacteria. Infect. Immun. **79**:203–210.
9. **Coats SR, Do CT, Karimi-Naser LM, Braham PH, Darveau RP.** 2007. Antagonistic lipopolysaccharides block E. coli lipopolysaccharide function at human TLR4 via interaction with the human MD-2 lipopolysaccharide binding site. Cell. Microbiol. **9**:1191–1202.
10. **Darveau RP, Arbabi S, Garcia I, Bainbridge B, Maier RV.** 2002. *Porphyromonas gingivalis* lipopolysaccharide is both agonist and antagonist for p38 mitogen-activated protein kinase activation. Infect. Immun. **70**: 1867–1873.
11. **Darveau RP, et al.** 2004. *Porphyromonas gingivalis* lipopolysaccharide contains multiple lipid A species that functionally interact with both Toll-like receptors 2 and 4. Infect. Immun. **72**:5041–5051.
12. **Folch J, Lees M, Sloane Stanley GH.** 1957. A simple method for the isolation and purification of total lipids from animal tissues. J. Biol. Chem. **226**:497–509.
13. **Garbus J, DeLuca HF, Loomas ME, Strong FM.** 1963. Rapid incorporation of phosphate into mitochondrial lipids. J. Biol. Chem. **238**:59–63.
14. **Gibson FC, III, et al.** 2004. Innate immune recognition of invasive bacteria accelerates atherosclerosis in apolipoprotein E-deficient mice. Circulation **109**:2801–2806.
15. **Gibson FC, III, Ukai T, Genco CA.** 2008. Engagement of specific innate immune signaling pathways during *Porphyromonas gingivalis* induced chronic inflammation and atherosclerosis. Front. Biosci. **13**:2041–2059.
16. **Hajishengallis G, et al.** 2002. Dependence of bacterial protein adhesins on toll-like receptors for proinflammatory cytokine induction. Clin. Diagn. Lab. Immunol. **9**:403–411.
17. **Hajishengallis G, Wang M, Bagby GJ, Nelson S.** 2008. Importance of TLR2 in early innate immune response to acute pulmonary infection with *Porphyromonas gingivalis* in mice. J. Immunol. **181**:4141–4149.
18. **Hajishengallis G, Wang M, Liang S.** 2009. Induction of distinct TLR2-mediated proinflammatory and proadhesive signaling pathways in response to *Porphyromonas gingivalis* fimbriae. J. Immunol. **182**:6690–6696.
19. **Harvey DJ.** 2009. Analysis of carbohydrates and glycoconjugates by matrix-assisted laser desorption/ionization mass spectrometry: an update for 2003–2004. Mass Spectrom. Rev. **28**:273–361.
20. **Hashimoto M, Asai Y, Ogawa T.** 2004. Separation and structural analysis of lipoprotein in a lipopolysaccharide preparation from *Porphyromonas gingivalis.* Int. Immunol. **16**:1431–1437.
21. **Hirschfeld M, Ma Y, Weis JH, Vogel SN, Weis JJ.** 2000. Cutting edge: repurification of lipopolysaccharide eliminates signaling through both human and murine Toll-like receptor 2. J. Immunol. **165**:618–622.
22. **Hirschfeld M, et al.** 2001. Signaling by Toll-like receptor 2 and 4 agonists results in differential gene expression in murine macrophages. Infect. Immun. **69**:1477–1482.
23. **Kumada H, Haishima Y, Umemoto T, Tanamoto K.** 1995. Structural study on the free lipid A isolated from lipopolysaccharide of *Porphyromonas gingivalis.* J. Bacteriol. **177**:2098–2106.
24. **Kumada H, et al.** 2008. Biological properties of the native and synthetic lipid A of *Porphyromonas gingivalis* lipopolysaccharide. Oral Microbiol. Immunol. **23**:60–69.
25. **Kussak A, Weintraub A.** 2002. Quadrupole ion-trap mass spectrometry to locate fatty acids on lipid A from Gram-negative bacteria. Anal. Biochem. **307**:131–137.
26. **Nichols FC.** 1994. Distribution of 3-hydroxy iC17:0 in subgingival plaque and gingival tissue samples: relationship to adult periodontitis. Infect. Immun. **62**:3753–3760.
27. **Nichols FC.** 1998. Novel ceramides recovered from *Porphyromonas gingivalis*: relationship to adult periodontitis. J. Lipid Res. **39**:2360–2372.
28. Reference deleted.
29. **Nichols FC, et al.** 2009. Unique lipids from a common human bacterium

represent a new class of Toll-like receptor 2 ligands capable of enhancing autoimmunity. Am. J. Pathol. **175**:2430–2438.
30. **Nichols FC, Maraj B.** 1998. Relationship between hydroxy fatty acids and prostaglandin $E_2$ in gingival tissue. Infect. Immun. **66**:5805–5811.
31. **Nichols FC, et al.** 2004. Structures and biological activity of phosphorylated dihydroceramides of *Porphyromonas gingivalis.* J. Lipid Res. **45**: 2317–2330.
32. **Nichols FC, Rojanasomsith K.** 2006. *Porphyromonas gingivalis* lipids and diseased dental tissues. Oral Microbiol. Immunol. **21**:84–92.
33. **Nichols FC, et al.** 2011. Phosphorylated dihydroceramides from common human bacteria are recovered in human tissues. PLoS One **6**:e16771.
34. **Ogawa T.** 1993. Chemical structure of lipid A from *Porphyromonas* (*Bacteroides*) *gingivalis* lipopolysaccharide. FEBS Lett. **332**:197–201.
35. **Ogawa T, Asai Y, Makimura Y, Tamai R.** 2007. Chemical structure and immunobiological activity of *Porphyromonas gingivalis* lipid A. Front. Biosci. **12**:3795–3812.
36. **Ogawa T, et al.** 2003. Endotoxic and immunobiological activities of a chemically synthesized lipid A of *Helicobacter pylori* strain 206-1. FEMS Immunol. Med. Microbiol. **36**:1–7.
37. **Ogawa T, et al.** 1997. Immunobiological activities of chemically defined lipid A from *Helicobacter pylori* LPS in comparison with *Porphyromonas gingivalis* lipid A and *Escherichia coli*-type synthetic lipid A (compound 506). Vaccine **15**:1598–1605.
38. **Reife RA, et al.** 2006. *Porphyromonas gingivalis* lipopolysaccharide lipid A heterogeneity: differential activities of tetra- and penta-acylated lipid A structures on E-selectin expression and TLR4 recognition. Cell. Microbiol. **8**:857–868.
39. **Safavi KE, Nichols FC.** 1993. Effect of calcium hydroxide on bacterial lipopolysaccharide. J. Endod. **19**:76–78.
40. **Sawada N, Ogawa T, Asai Y, Makimura Y, Sugiyama A.** 2007. Toll-like receptor 4-dependent recognition of structurally different forms of chemically synthesized lipid As of *Porphyromonas gingivalis.* Clin. Exp. Immunol. **148**:529–536.
41. **Shaffer SA, Harvey MD, Goodlett DR, Ernst RK.** 2007. Structural heterogeneity and environmentally regulated remodeling of *Francisella tularensis* subspecies *novicida* lipid A characterized by tandem mass spectrometry. J. Am. Soc. Mass Spectrom. **18**:1080–1092.
42. **Triantafilou M, et al.** 2007. Lipopolysaccharides from atherosclerosis-associated bacteria antagonize TLR4, induce formation of TLR2/1/CD36 complexes in lipid rafts and trigger TLR2-induced inflammatory responses in human vascular endothelial cells. Cell. Microbiol. **9**:2030–2039.
43. **Wang YH, et al.** 2010. *Porphyromonas gingivalis* lipids inhibit osteoblastic differentiation and function. Infect. Immun. **78**:3726–3735.
44. **Wesphal O, Jann K.** 1965. Bacterial lipopolysaccharides: extraction with phenol-water and further applications of the procedure, p 83–91. *In* Whistler RL (ed), Methods in carbohydrate chemistry, vol 5. Academic Press Inc., New York, NY.
45. **Xu N, Huang ZH, de Jonge BL, Gage DA.** 1997. Structural characterization of peptidoglycan muropeptides by matrix-assisted laser desorption ionization mass spectrometry and postsource decay analysis. Anal. Biochem. **248**:7–14.
46. **Yi EC, Hackett M.** 2000. Rapid isolation method for lipopolysaccharide and lipid A from gram-negative bacteria. Analyst **125**:651–656.
47. **Zhang P, et al.** 2011. TLR2-dependent modulation of osteoclastogenesis by *Porphyromonas gingivalis* through differential induction of NFATc1 and NF-{kappa}B. J. Biol. Chem. **286**:24159–24169.
48. **Zhou P, Altman E, Perry MB, Li J.** 2010. Study of matrix additives for sensitive analysis of lipid A by matrix-assisted laser desorption ionization mass spectrometry. Appl. Environ. Microbiol. **76**:3437–3443.